

# FOCUSING SAR DATA ACQUIRED FROM NON-LINEAR SENSOR TRAJECTORIES

*Othmar Frey, Christophe Magnard, Maurice Rüegg and Erich Meier*

Remote Sensing Laboratories  
University of Zurich, Switzerland

## ABSTRACT

Standard focusing of SAR data assumes a straight recording track of the sensor platform. Small non-linearities of airborne platform tracks are corrected for during a motion compensation step while keeping the assumption of a linear flight path. In the following, the processing of SAR data from *non-linear* tracks is discussed as may originate from small aircraft or drones flying at low altitude. They fly not a straight track but one dependent on topography, influences of weather and wind, or dependent on the shape of dedicated areas of interest such as rivers or traffic routes. A time-domain back-projection based technique, is proposed and evaluated with the help of experimental data featuring a drop in height, a double bend, a 90-degree curve and a linear flight track. In order to assess the quality of the focused data, close-ups of amplitude images are compared and the coherence is evaluated. The experimental data was acquired by the German Aerospace Center's E-SAR L-band system.

## 1. INTRODUCTION

SAR systems mounted on small aircraft or drones may exhibit highly non-linear flight paths, to an extent that a model of a linear sensor trajectory no longer holds. This scenario may occur due to various factors such as rugged topography, atmospheric turbulence, but also due to the need for more flexibility in mission design as, for instance, for airborne or drone-based monitoring of curvilinear areas of interest (corridor mapping), such as rivers and nearby (potential) flooding areas or traffic routes.

In such cases, the model assumption of one linear trajectory, upon which the standard frequency domain processing methods [1, 2, 3] are based, is not sufficient, and therefore more flexible processing approaches must be sought.

In [4] the problem of processing SAR data from non-linear flight tracks is treated in some detail and two solutions are proposed. The first solution is processing the data by time-domain back-projection. However, the problem is again described with the help of a two-dimensional formulation of the problem similar to the formulation presented in [5] and there is no remark with respect to how the changing Doppler centroid frequency is handled over azimuth. The second solution,

which is proposed, is a  $\omega - k$ -based subaperture processing algorithm which is claimed to give superior results compared to the time-domain back-projection approach. Unfortunately, neither of these publications comes up with results obtained with real SAR data from highly non-linear flight tracks.

We aim at filling this gap by, first, presenting an algorithm, which handles the azimuth-varying pointing direction of the antenna as well as the arbitrary flight path, and, second, by proofing the fitness of our TDBP algorithm using real-world experimental data acquired from highly non-linear flight tracks.

## 2. TDBP PROCESSING OF NON-LINEAR SAR DATA

Our TDBP implementation has been described in [6, 7]. Here, we mainly focus on the extension that makes the algorithm suitable to process synthetic aperture radar data acquired from an arbitrary flight track. The key items of the TDBP approach which enable successful processing of such raw data are the following:

By processing the data in the time-domain we can exploit the exact three-dimensional configuration (to the extent that the motion of the aircraft is accurately measured) of the acquisition pattern and the surface of the illuminated area.

The Doppler centroid frequency is determined from the sensor's velocity, position and attitude data and is updated for each radar echo.

The varying boundaries of the Doppler bandwidth over azimuth are compared to the Doppler frequency under which the individual target points are "seen". The signal contributions to a certain point on the reconstruction grid are weighted according to the Doppler frequency or omitted if the Doppler frequency exceeds the Doppler boundaries.

The scene is divided into a user-defined number of patches that can be processed in parallel. The Doppler centroid frequency  $f_{dc_j}$  is calculated from the navigational data for each radar echo:

$$f_{dc_j} = \frac{2}{\lambda_c} \cdot \vec{v}_{S_j} \cdot \vec{u}_{P_j}, \quad (1)$$

where  $\lambda_c$  is the wave length of the carrier signal,  $\vec{v}_{S_j}$  is the velocity vector of the sensor corresponding to the  $j$ -th radar echo and  $\vec{u}_{P_j}$  is the unit vector in direction where the antenna

is pointing to.  $\vec{u}_{P_j}$  is calculated from the sensors positioning and attitude data (roll, pitch and heading) and is updated for each radar echo. Using  $f_{dc_j}$  the azimuth-varying upper and lower limit of the Doppler bandwidth to process yield  $f_{d_{max_j}} = f_{dc_j} + f_B/2$  and  $f_{d_{min_j}} = f_{dc_j} - f_B/2$ , where  $f_B$  is the constant absolute Doppler bandwidth.

For each pixel on the reconstruction grid the Doppler frequency  $f_{d_{ij}}$  is calculated based on the varying geometric constellation given by the position vector on the ground  $\vec{r}_i$ , the position vector  $\vec{r}_{S_j}$  and velocity vector  $\vec{v}_{S_j}$  of the sensor:

$$f_{d_{ij}} = \frac{2}{\lambda_c} \cdot \frac{\vec{v}_{S_j} \cdot (\vec{r}_i - \vec{r}_{S_j})}{|\vec{r}_i - \vec{r}_{S_j}|} \quad (2)$$

During the coherent summation in the time domain a weighting function  $w(df_{d_{ij}})$  is applied, where  $df_{d_{ij}} = f_{d_{ij}} - f_{dc_j}$ . The weighting term  $w$  ensures that only signal contributions according to the actual orientation of the sensor at each azimuth time step are coherently added:

$$w(df_{d_{ij}}) = \begin{cases} \alpha - (1 - \alpha) \cos\left(\frac{2\pi df_{d_{ij}}}{B} - \pi\right) & , |df_{d_{ij}}| \leq \frac{B}{2} \\ 0 & , |df_{d_{ij}}| > \frac{B}{2} \end{cases} \quad (3)$$

Eventually, the weighting function in eq. (3) is incorporated in the TDBP focusing algorithm and we obtain the focused signal  $s(\vec{r}_i)$ :

$$s(\vec{r}_i) = \sum_{j=a(\vec{r}_i)}^{b(\vec{r}_i)} w(df_{d_{ij}}) \cdot g(|\vec{r}_i - \vec{r}_{S_j}|, \vec{r}_{S_j}) \cdot |\vec{r}_i - \vec{r}_{S_j}| \cdot \exp(j2k_c |\vec{r}_i - \vec{r}_{S_j}|) \quad (4)$$

$a$  and  $b$  are the indices of the first and last sensor position, respectively, the echo of which still contributes to the grid position  $\vec{r}_i$ .  $g(\cdot)$  is the range-compressed, demodulated two-way response and  $k_c$  is the central wavenumber.

### 3. DESCRIPTION OF THE EXPERIMENT

In order to assess the performance of the proposed TDBP approach with real data four tracks have been flown by the German Aerospace Center's E-SAR system: a quasi-linear reference track, a drop in height of approx. 250 m (*dive*), a double bend and a 90-degree curve flight as depicted in Fig. 1.

The system parameters of the used L-band sensor are listed in Table 1. Besides the focusing quality, the geometric fidelity of the final image is an important point for the user. In order to be able to assess the preservation of dedicated features in the focused image an airfield has been chosen as our test site. On the airfield a lot of linear elements like a runway and fences and large buildings are present.

### 4. RESULTS

All four data sets have directly been focused onto a reconstruction grid based on a digital elevation model in map ge-

Carrier frequency	1.3 GHz
Chirp bandwidth	94 MHz
Sampling rate	100 MHz
PRF	400 Hz
Ground speed	90 m/s
Azimuth beam width	18°
Elevation beam width	35°
Look direction	left

**Table 1.** E-SAR L-Band System Specifications.

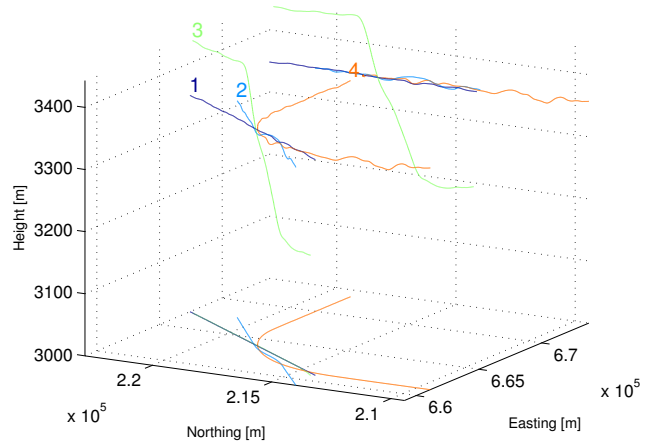


**Fig. 1.** Non-linear flight tracks flown during the experiment as obtained from the DGPS/INS unit of the E-SAR system: 1. Quasi-linear reference track, 2. double bend, 3. dive, 4. 90-degree curve.

ometry. In Fig. 2 a common area that was illuminated during all four data takes is depicted. A high focusing quality within the whole area is achieved and all linear features, as for instance the runway, are well-preserved in all cases regardless of the geometry of the flight path.

This is the result of keeping track of the three-dimensional geometry during the focusing step. Further, the weighting function ensures that the varying looking direction of the antenna is accounted for thereby eliminating ghost targets. The small variations in the four images are due to different look directions. The most noticeable difference is obviously given for the 90-degree curvilinear track where strong back-scattering of targets perpendicular to the flight track is practically eliminated by the change in the direction of illumination. In order to illustrate the flexibility of our processing approach the whole data strip for the curvilinear acquisition mode is depicted in Fig. 3. Again, the image is given in map coordinates (easting/northing). The geometric fidelity is high in all cases, which is indicated by the fact that linear features,

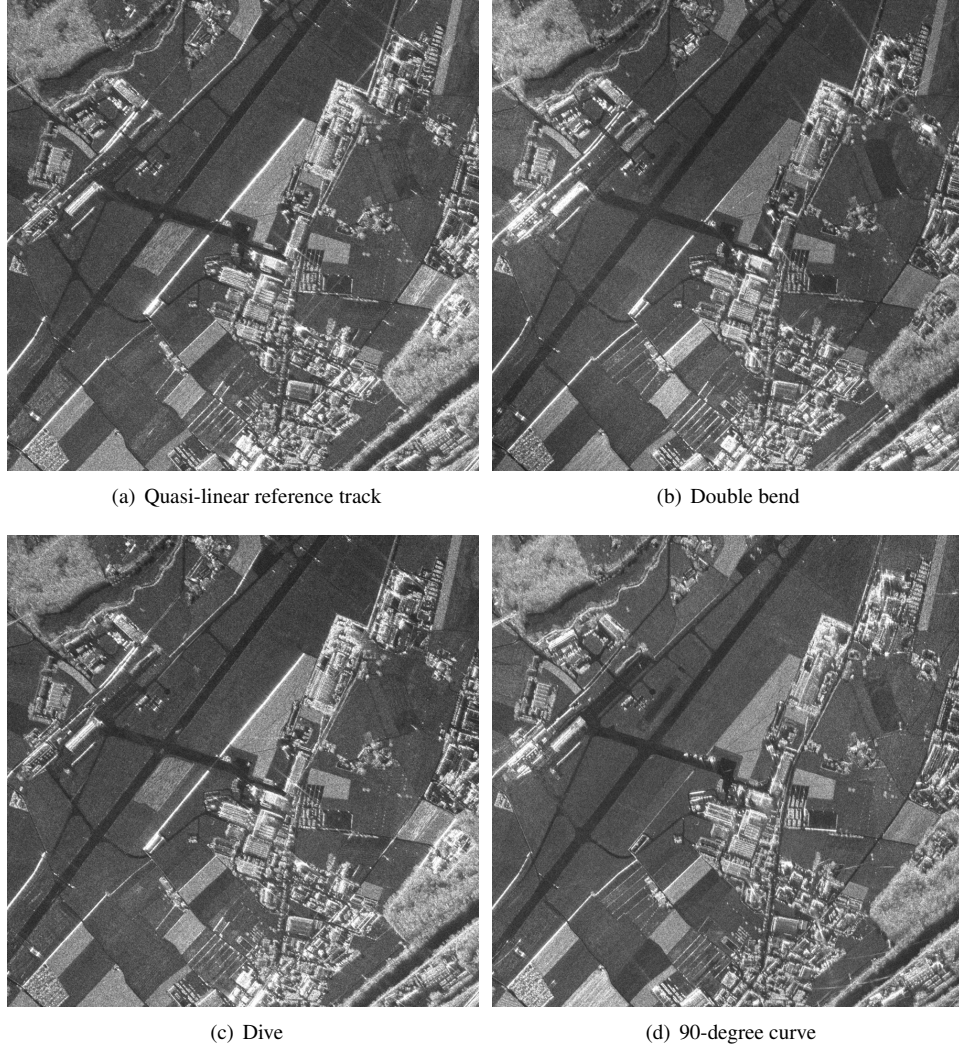


**Fig. 2.** Detail of a common area in all four experimental data sets. Sensor: E-SAR L-band HH. (a) quasi-linear reference track, (b) double bend, (c) dive, and (d) 90-degree curve. The data sets were focused on a DEM-based reconstruction grid in map geometry by time-domain back-projection processing.

such as the runway and fences, are well-preserved. In order to illustrate the processing quality the coherence map for the data pair *reference track/dive* is given in Fig. 4. Note that the coherence is not optimized in the sense that the Doppler and range spectra are reduced to their common spectral band. The reason is that we only want to use the coherence as another indicator for the processing quality. High coherence values are obtained for a small region where the flight tracks are well within the critical baseline and where the look direction is similar.

## 5. CONCLUSION

We have demonstrated that the time-domain back-projection based algorithm, which is proposed in this paper, is suitable

to produce high-quality images for airborne SAR data from highly non-linear flight tracks. A high focusing quality is achieved regardless of the acquisition geometry. And as a natural side-effect of the back-projection algorithm accurately geo-referenced complex-valued SAR images are obtained. The processing technique allows a flexible and parallelized processing even of dedicated subareas of interest within a dataset acquired from virtually arbitrarily shaped flight tracks thereby increasing the flexibility for mapping of curvilinear features like rivers or traffic routes.

## 6. REFERENCES

- [1] Alberto Moreira and Yonghong Huang, "Airborne SAR Processing of Highly Squinted Data Using a Chirp Scal-

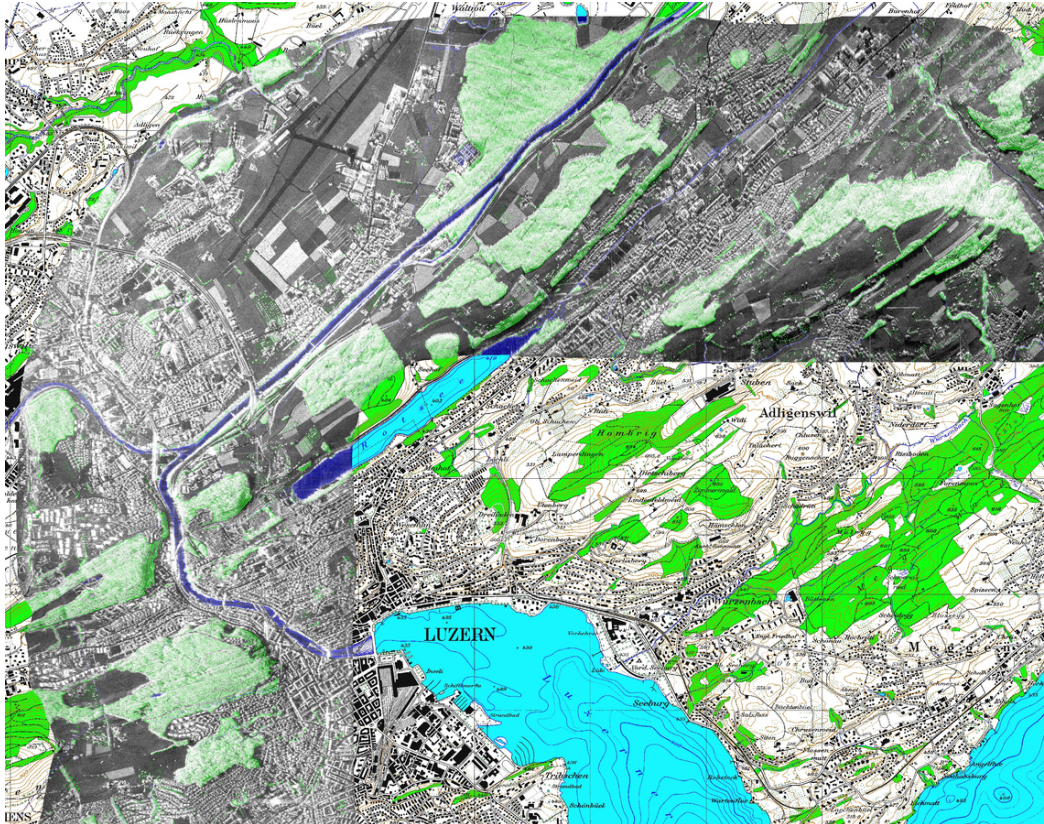


**Fig. 3.** Amplitude image of the 90-degree curve track: E-SAR L-band HH. Processing: TDBP. The data set has been processed directly to map coordinates using a digital elevation model. The SAR amplitude image is blended with a 1:25000 scale digital map of the area. Map reproduced by permission of swisstopo (BA081196).

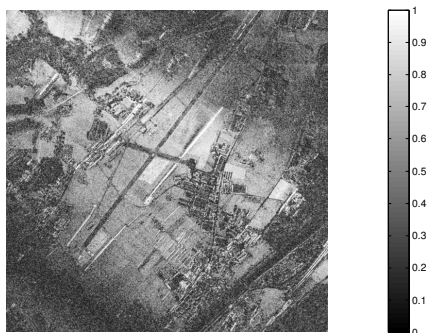


**Fig. 4.** Coherence map for the pair dive/reference track processed by TDBP. See Fig. 1 for the corresponding sensor trajectories.

ing Approach with Integrated Motion Compensation,” *IEEE Trans. Geosci. Remote Sensing*, vol. 32, no. 5, pp. 1029–1040, Sept. 1994.

[2] R. Keith Raney, Hartmut Runge, Richard Bamler, Ian G. Cumming, and Frank H. Wong, “Precision SAR Process-

ing Using Chirp Scaling,” *IEEE Trans. Geosci. Remote Sensing*, vol. 32, no. 4, pp. 786–799, July 1994.

[3] Ciro Cafforio, Claudio Prati, and Fabio Rocca, “SAR Data Focusing Using Seismic Migration Techniques,” *IEEE Trans. Aerosp. Electron. Syst.*, vol. 27, no. 2, pp. 194–207, Mar. 1991.

[4] Mehrdad Soumekh, “Time Domain Non-Linear SAR Processing,” Tech. Rep., Department of Electrical Engineering, State University of New York, 2006.

[5] Mehrdad Soumekh, *Synthetic Aperture Radar Signal Processing: with MATLAB Algorithms*, John Wiley & Sons, 1999.

[6] Othmar Frey, Erich Meier, and Daniel Nüesch, “An Integrated Focusing and Calibration Procedure for Airborne SAR Data,” in *Proc. EUSAR*, Dresden, Germany, May 2006, pp. 1–4.

[7] Othmar Frey, Erich Meier, and Daniel Nüesch, “Processing SAR Data of Rugged Terrain by Time-Domain Back-Projection,” in *Proc. SPIE*, Bruges, Belgium, Sept. 2005, vol. 5980, pp. 1–9.